Dynamic light scattering from a highly swollen nonionic lamellar liquid crystal

C. Y. Zhang, S. Sprunt, and J. D. Litster
Department of Physics and Francis Bitter National Magnet Laboratory, Massachusetts Institute of Technology, Cambridge, Massachusetts 02139-4307
(Received 16 February 1993)

We have conducted a dynamic light-scattering study of the homeotropically aligned highly swollen lamellar phase (layer separation $d \sim 180$ nm) of a nonionic binary system, dodecylpentaglycol (C12E5) and water, where the steric and entropic repulsion is the dominant intermembrane force stabilizing the lamellar order. We have identified a hydrodynamic mode in the two momentum-transfer limits available to light scattering. Based on previous models, we have found an explicit expression for the dispersion relation of this "baroclinic" or "slip" mode for systems with large layer spacing, which successfully explains our experimental results. When d is large, the bilayer curvature elasticity and the viscous coupling between water and the bilayers become more important to the understanding of the baroclinic mode. We found the curvature elastic constant $k_c \simeq k_B T$, consistent with generally accepted values for flexible membranes.

PACS number(s): 61.30.Cz, 61.30.Eb, 78.35.+c

I. INTRODUCTION

Certain lyotropic smectic liquid crystals can be diluted to a very large extent without loss of their smectic order. For example, a quaternary system containing sodium dodecyl sulfate (SDS) can be swollen to a layer spacing d greater than 50 nm [1,2], while a similar system containing octyl benzene sulfonic salt (OBS) can be swollen to $d \sim 500$ nm [3]. A simple binary mixture of the nonionic surfactant dodecylpentaglycol (C12E5) and water has been diluted to 99 wt. % water, yielding a lamellar phase with a layer spacing exceeding 300 nm [4]. A sketch of the structure of the C12E5-water lamellar phase is shown in Fig. 1. The surfactant forms bilayers with thickness $\zeta = 3.75$ nm [4]; geometrically, d is determined by the surfactant volume fraction ϕ according to the simple relation $d \simeq \zeta/\phi$. In systems with $d \gg 10$ nm, the short-range hydration and Van der Waals interactions between bilayers are unimportant. There is a long-range electrostatic interaction in the ionic systems of SDS or OBS, but by choosing an oil dilution or brine dilution, this interaction can be reduced [2]. For the nonionic system of C12E5, there is no significant electrostatic interaction. The dominant force to stabilize the smectic order is the entropic and steric repulsion between layers, first proposed by Helfrich [5]. The free energy per unit area of bilayer due to this interaction is

$$V_h = \frac{3\pi^2}{128} \frac{(k_B T)^2}{k_c d^2} \tag{1}$$

where k_c is the curvature elasticity of the bilayer.

In this paper, we report the results of a dynamic light scattering study of the very dilute L_α phase in the nonionic C12E5 system. We also discuss our results by extending a model of the hydrodynamics for a lipid-water lamellar phase. The model was originally formulated by Brochard and de Gennes [6] and has been further developed by Nallet, Roux, and Prost [7] in the course of analyzing their experiments on the SDS system. In treating the energy involved in bilayer deformation, Brochard and de Gennes assumed a stretching in the plane of the layers, producing a change in the area per surfactant molecule. Nallet *et al.* introduced a layer compression which results in a change in bilayer thickness. In both approaches, the usual five variables of a simple fluid (the mass, momentum, and energy densities) are supplemented by two other hydrodynamic variables [9], for example, the bilayer displacement u and the surfactant concentration c. While the description of the resulting seven hydrodynamic modes can be complicated, the problem becomes simpler with reasonable assumptions [6,7]. In particular, when the wave vector is oblique with respect to the layers, one obtains a slip [6] or baroclinic [7] mode, whose approximate dispersion relation is

$$\omega = -i\mu D_{22} q_\perp^2 \tag{2}$$

where

$$D_{22} = d\frac{\partial^2 V_h}{\partial d^2} = \frac{9\pi^2}{64} \frac{(k_B T)^2}{k_c d^3} , \tag{3}$$

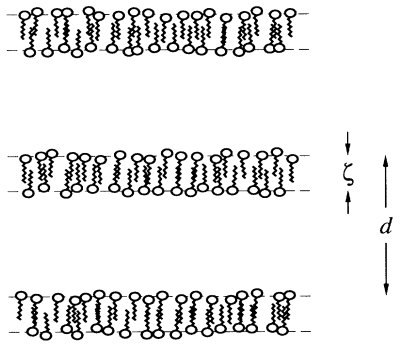

FIG. 1. A sketch of the structure of a swollen lyotropic smectic liquid crystal.

μ is the slip coefficient [6], k_c is the curvature elastic constant for a bilayer, and $q_\perp$ is the component of $\mathbf{q}$ perpendicular to the normal to the bilayers. For $d \gg \zeta$, one expects [6] $\mu = d^2/(12\eta)$, where η is the viscosity of water. The baroclinic mode involves fluctuations in the concentration of surfactant, and can scatter light rather strongly. To discuss the scattering, let $\mathbf{i}$ and $\mathbf{f}$ denote the polarizations of the incident and scattered light. Also let $\mathbf{n}$ be the director (optic axis) and c be the concentration (number of molecules per unit volume) of the surfactant molecules; in terms of their fluctuating components, these may be written $\mathbf{n} = \mathbf{n}_0 + \delta\mathbf{n}$ and $c = c_0 + \delta c$, where $\mathbf{n}_0$ and c_0 are equilibrium values. The intensity of scattered light is given by [7]

$$
\begin{aligned}
I(\mathbf{q}) &\sim \int \exp(i\mathbf{q}\cdot\mathbf{r}) \langle \delta\epsilon^*_{if}(0)\delta\epsilon_{fi}(\mathbf{r})\rangle d\mathbf{r} \\
&= (\partial\bar{\epsilon}/\partial c)^2(\mathbf{i}\cdot\mathbf{f})^2 S_{cc}(\mathbf{q}) + \epsilon_a^2[(\mathbf{n}_0\cdot\mathbf{i})(\mathbf{q}_\perp\cdot\mathbf{f}) + (\mathbf{n}_0\cdot\mathbf{f})(\mathbf{q}_\perp\cdot\mathbf{i})]^2 S_{uu}(\mathbf{q}) \\
&\quad + (\partial\bar{\epsilon}/\partial c)\epsilon_a(\mathbf{i}\cdot\mathbf{f})[(\mathbf{n}_0\cdot\mathbf{i})(\mathbf{q}_\perp\cdot\mathbf{f}) + (\mathbf{n}_0\cdot\mathbf{f})(\mathbf{q}_\perp\cdot\mathbf{i})][S_{cu}(\mathbf{q}) - S^*_{cu}(\mathbf{q})] \, . \qquad (4)
\end{aligned}
$$

The surfactant molecular dielectric tensor is ϵ, $\bar{\epsilon} = (\epsilon_\parallel + 2\epsilon_\perp)/3$, and $\epsilon_a = \epsilon_\parallel - \epsilon_\perp$. As ϵ_a is very small, higher-order terms have been neglected:

$$S_{cc}(\mathbf{q}) = \int \exp(i\mathbf{q}\cdot\mathbf{r}) \langle \delta c^*(0)\delta c(\mathbf{r})\rangle d\mathbf{r} \, , \qquad (5a)$$

$$S_{uu}(\mathbf{q}) = \int \exp(i\mathbf{q}\cdot\mathbf{r}) \langle \delta u^*(0)\delta u(\mathbf{r})\rangle d\mathbf{r} \, , \qquad (5b)$$

$$S_{cu}(\mathbf{q}) = \int \exp(i\mathbf{q}\cdot\mathbf{r}) \langle \delta c^*(0)\delta u(\mathbf{r})\rangle d\mathbf{r} \, . \qquad (5c)$$

From this we can see that concentration fluctuations contribute to light scattering through the first and the third terms of Eq. (4).

II. EXPERIMENT

The C12E5 was obtained from Fluka and used without further purification. The water was triply distilled. The sample was made of 2.0 wt. % C12E5 and 98 wt. % water; this gives a lamellar spacing $d \sim 180$ nm [4]. It was loaded in the isotropic L_1 phase into a cell made of two fused silica plates separated by a 0.4-mm teflon spacer which also served as a gasket to seal the cell. A homeotropic well-aligned single-domain lamellar phase was obtained by filling the cell at room temperature, then rapidly heating to the upper L_α phase and allowing it to equilibrate for 24 hours; then the sample was heated into the isotropic phase and slowly cooled back into the L_α phase. When examined under a microscope, the sample showed a uniform texture and good optical extinction between crossed polarizers. During the experiment, the temperature was kept at $T = 59\,^\circ$C, in the upper L_α phase. The light scattering setup is shown schematically in Fig. 2. We chose the z axis parallel to the normal to the bilayers, and the x axis in the scattering plane so that $q_\parallel = q_z$ and $q_\perp = q_x$. To isolate the concentration fluctuations, both polarizations $\mathbf{i}$ and $\mathbf{f}$ were set perpendicular to the plane of scattering, so that the bracketed geometric factor contained in the second and the third terms of Eq. (4) equaled zero. The sample was illuminated by a helium-neon laser ($\lambda = 6328$ Å). The scattered light was collected at 13 angles ranging from $\theta = 9°$ to 43° inside the sample. Strong signals were obtained with a signal-to-background ratio of at least 1/5. By comparing the intensity autocorrelation function to that from a solution of standard polystyrene latex spheres in the same scattering geometry, we determined the scattering to be homodyne. Typical correlation functions are plotted in Fig. 3. All of the correlation functions can be fitted very well with two decay times, a larger amplitude slow mode and a smaller amplitude fast mode. The fitting function was

$$y = B + [A_1 \exp(-\Gamma_1 t) + A_2 \exp(-\Gamma_2 t)]^2 \qquad (6)$$

with B fixed at the measured background. The values for Γ_1 and Γ_2 are plotted vs q_x in Fig. 4; both modes appeared to depend linearly on q_x^3. If we associate the slow mode (Γ_1) with the baroclinic mode described by Eqs. (2) and (3), we obtain $D_{22} = 0.36$ Pa from the slope of the fit to q_x^2, and find $k_c = 2.8 k_B T$ from Eq. (3). While these values compare well with those obtained by Nallet, Roux, and Prost [7] from studying the baroclinic mode of the SDS system, where the range of swelling was from 3 to 35 nm, k_c is two to three times the value obtained for a similar C12E5 system by Strey *et al.* [4] by studying thermally induced deviations from linear swelling with $d = \zeta/\phi$. It is also about three times the value obtained by Nallet, Roux, and Prost from their study of the undulation mode. This disagreement leads us to reconsider, for the particular case of a system with very larger d, the hydrodynamics of the baroclinic mode. As a result, we shall obtain a more complete expression for the dispersion relation Eq. (2). We shall also explain the origin of the two decay times observed at each scattering angle.

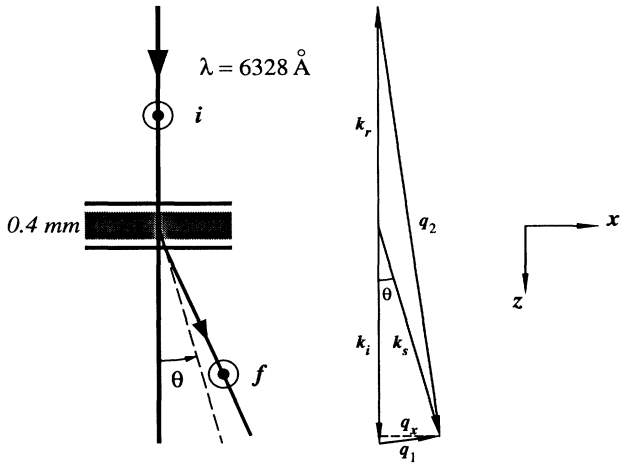

FIG. 2. Geometry of the light-scattering experiment.

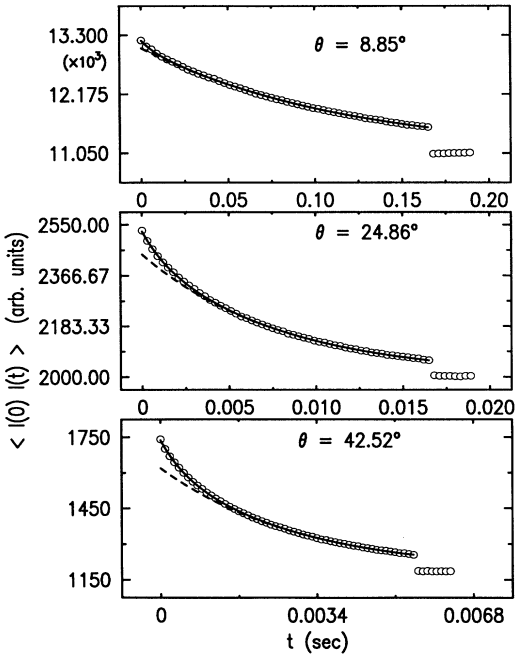

FIG. 3. Typical intensity autocorrelation functions for the scattered light and fits to Eq. (6). The dashed lines show the decay of the slow mode only.

III. HYDRODYNAMICS OF THE LAMELLAR PHASE

To discuss the hydrodynamics of the binary lipid system for large d, we use the phenomenological approach of Brochard and de Gennes for lyotropic smectics [6]. Our notation is that of Ref. [6]; in an appendix we give a table translating to the notation of Ref. [7]. At constant temperature we need three variables to describe the interesting behavior of the lamellar phase. These may be the total density dilation Θ, the dilation of the layer spacing $\gamma=(d-d_{\rm eq})/d_{\rm eq}=\partial u/\partial z$, and the dilation of the surfactant concentration $\varepsilon=(c_0-c)/c_0=\partial c/c_0$ where $d_{\rm eq}$ is the layer spacing at equilibrium. Since Θ involves the first sound, which is much faster than the membrane fluctuations we are considering and couples little to them, we may assume the material is incompressible. For the third variable, instead of using ε, one may use the relative change of the area per polar head $\delta=(A-A_{\rm eq})/A_{\rm eq}$ where $A_{\rm eq}$ is the area per polar head at equilibrium. These are related by $\varepsilon=\gamma+\delta$. Using strain of the area of surfactant molecules as one of our variables is similar to a more recent approach by Lubensky, Prost, and Ramaswamy [8] where a crumpling membrane is introduced. The free energy density can therefore be expanded as

$$f=\tfrac{1}{2}D_{22}\gamma^2+D_{23}\gamma\delta+\tfrac{1}{2}D_{33}\delta^2+\tfrac{1}{2}K\left[\frac{\partial^2 u}{\partial x^2}\right]^2$$
$$\equiv f_1+\tfrac{1}{2}K\left[\frac{\partial^2 u}{\partial z^2}\right]^2, \tag{7}$$

where the last term is the membrane curvature elastic energy and $K=k_c/d$. Following [6], the equations of motion of the fluid are

$$\rho\frac{\partial v_x}{\partial t}=-\frac{\partial p}{\partial x}+\frac{\partial}{\partial x}\left[\frac{\partial f_1}{\partial\delta}\right]_\gamma+\eta\left[2\frac{\partial^2 v_x}{\partial x^2}+\frac{\partial^2 v_x}{\partial z^2}+\frac{\partial^2 v_z}{\partial x\,\partial z}\right], \tag{8}$$

$$\rho\frac{\partial v_z}{\partial t}=-\frac{\partial p}{\partial z}+\frac{\partial}{\partial z}\left[\frac{\partial f_1}{\partial\gamma}\right]_\delta-K\left[\frac{\partial^4 u}{\partial x^4}\right]+\eta\left[2\frac{\partial^2 v_z}{\partial z^2}+\frac{\partial^2 v_z}{\partial x^2}+\frac{\partial^2 v_x}{\partial x\,\partial z}\right], \tag{9}$$

where we have included the force due to curvature elasticity, and p and $\mathbf{v}$ are the local pressure and velocity of the fluid. Water is assumed not to cross the bilayers, and the surfactant molecules are assumed not to leave them; that is, no permeation occurs. With no permeation $v_z=\partial u/\partial t$, and the x component of the lipid velocity is given by $v_{Lx}=\partial\delta/\partial t$. Under these conditions, and with the material 98% water, it is appropriate to use an isotropic shear viscosity η equal to the viscosity of water in Eqs. (8) and (9). (Equations including permeation and anisotropic expressions for the shear viscosity can be found in [6] and [7].) Water may, however, flow between the bilayers in the x direction. This is described by the phenomenological equation [6]

$$(v_{Lx}-v_x)=\mu\frac{\partial}{\partial x}\left[\frac{\partial f_1}{\partial\delta}\right]_\gamma, \tag{10}$$

where v_{Lx} is the x component of lipid velocity. Then we may combine $\nabla\cdot\mathbf{v}_L=\partial\varepsilon/\partial t$ with the incompressibility condition $\nabla\cdot\mathbf{v}=0$ to obtain

$$\frac{\partial\varepsilon}{\partial t}=\mu\frac{\partial^2}{\partial x^2}\left[\frac{\partial f_1}{\partial\delta}\right]_\gamma. \tag{11}$$

If we assume the Fourier components of u and ε have the time and space dependence $e^{i\mathbf{q}\cdot\mathbf{r}-i\omega t}$ we may use Eqs. (9)

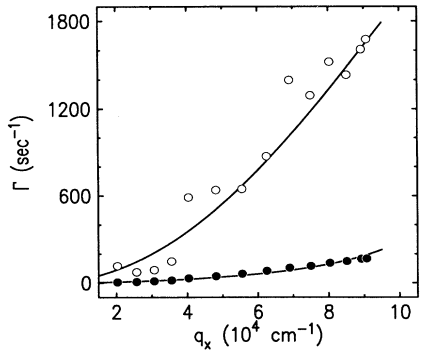

FIG. 4. Fits of the slow and fast decay times to Eq. (12). The open circles are forward scattering (fast decay) and the filled circles are backward scattering (slow decay).

and (11), combined with the incompressibility and impermeability conditions to arrive at the characteristic determinant for nontrivial u and ε:

$$(\omega^2-i\omega\eta q^2/\rho-\omega_0^2)(i\omega+\mu q_x^2 D_{33})-\omega_1^2(i\omega+\mu q_x^2 D_{23})=0, \tag{12}$$

where

$$\omega_0^2=\frac{1}{\rho}\left[\frac{q_x q_z}{q}\right]^2\left[D_{22}-D_{23}+K\frac{q_x^4}{q_z^2}\right], \tag{13a}$$

$$\omega_1^2=\frac{1}{\rho}\left[\frac{q_x q_z}{q}\right]^2(D_{33}-D_{23}). \tag{13b}$$

Before solving Eq. (12), it is useful to estimate the magnitudes of D_{22}, D_{23}, and D_{33}. Physically, f_1 in Eq. (7) arises from the effects of the Helfrich repulsion and layer stretching; these may be described by the phenomenological free energy density

$$\mathcal{F}=\frac{V_h(d)}{d_{\rm eq}}+\tfrac{1}{2}\chi c(A-A_0)^2, \tag{14}$$

where χ is a coefficient of layer resistance to stretching [6] and A_0 is the area per polar head in an unstretched bilayer. In order to expand $\mathcal{F}$ in terms of γ and δ, let us imagine a static process (with no long-range fluctuations) in which such bilayers are assembled to a lamellar phase of separation d_0. The concentration of surfactant will be $c_0=2/A_0 d_0$ molecules per unit volume. When such a lamellar phase relaxes to equilibrium, the repulsion between the layers will cause an increase in layer spacing to $d_{\rm eq}=d_0(1+\gamma_0)$; we expect $\gamma_0\ll 1$. Since the surfactant concentration does not change during this process, $A_{\rm eq}d_{\rm eq}=A_0 d_0$ and there will be a corresponding reduction of A to $A_{\rm eq}=A_0/(1+\gamma_0)$. To find γ_0, we minimize $\mathcal{F}$ while keeping both the surfactant concentration fixed at c_0 and the number of layers fixed. This requires

$$\frac{1}{d_{\rm eq}}\frac{\partial V_h(d)}{\partial d}+\tfrac{1}{2}\chi c_0 A_0^2\frac{\partial}{\partial d}(1-d_0/d)^2=0. \tag{15}$$

The solution to Eq. (15) gives the value for $d_{\rm eq}$, from which we may calculate γ_0, $A_{\rm eq}$, and $\mathcal{F}_{\rm eq}$. The result is $\gamma_0\simeq V_h/\chi A_{\rm eq}$. With $\gamma+\delta+\gamma\delta=0$ to maintain constant surfactant concentration, we calculate

$$f_1=\mathcal{F}(\gamma,\delta)-\mathcal{F}_{\rm eq}$$
$$=\frac{9\pi^2}{12k}\frac{(k_B T)^2}{k_c d_{\rm eq}^3}\gamma^2+\chi c_0 A_{\rm eq}^2\gamma_0\gamma\delta+\tfrac{1}{2}\chi c_0 A_{\rm eq}^2\delta^2. \tag{16}$$

Thus,

$$D_{22}=\frac{9\pi^2}{64}\frac{(k_B T)^2}{k_c d_{\rm eq}^3}, \tag{17}$$

$$D_{33}=\chi c_0 A_{\rm eq}^2=2\chi A_{\rm eq}/d_{\rm eq}, \tag{18}$$

and

$$D_{23}=\chi c_0 A_{\rm eq}^2\gamma_0=2V_h/d_{\rm eq}=D_{22}/3. \tag{19}$$

The cross term D_{23} arises because in equilibrium each bilayer is slightly compressed in order to reduce the repulsion between the layers. For our system with $d_{\rm eq}\simeq 180$ nm, and $k_c\sim k_B T=4.58\times10^{-12}$ nJ, we estimate $D_{22}\sim 0.8$ Pa, or 8 erg cm^{-3}. We might naively estimate D_{33} using typical values [10] for $\chi\simeq 2\times10^{18}$ Pa m^{-1} and $A_{\rm eq}\simeq 0.6$ nm^2; for our sample we would obtain $D_{33}\simeq 1.2\times10^6$ Pa, or 1.2×10^7 erg cm^{-3}. However, the large thermal fluctuations responsible for the Helfrich force mean that the layers are substantially crumpled, although flat on average at long wavelengths. The coefficient D_{33} is therefore greatly reduced, in the same way that crepe paper is much easier to stretch than smooth paper. The magnitude of this effect has been calculated by Lubensky, Prost, and Ramaswamy [8], who estimate $D_{33}\sim 200$–$400 D_{22}$, that is, $D_{33}\simeq 160$–320 Pa. This leads to $\gamma_0\simeq 2\times10^{-3}$, which is indeed $\ll 1$ is assumed.

We now return to solve Eq. (12). There are three roots to the cubic equation and it is not easy to find the analytical solutions to all of them. Our first approach is to find the purely imaginary root which has the lowest frequency, in order to explain the diffusive modes in our experiment. It turns out that when $D_{33}\gg D_{22}, D_{23}$ and $\omega\le 10^3$ sec^{-1} we can drop the terms in Eq. (12) which contain ω^2 and ω^3. We then obtain

$$i\omega=\Gamma=\mu\frac{D_{22}q_z^2+Kq_x^4}{q_z^2+\mu\eta q^4+(K/D_{33})q_x^4}q_x^2. \tag{20}$$

If q_z is not too small this expression crosses over to Eq. (2) as d becomes smaller. That is because μ and the ratio K/D_{22} are proportional to d^2 and the K/D_{33} term in the denominator is not very important. It becomes a mode of layer undulation when $q_z\to 0$. The relative amounts of layer displacement u and concentration change ε, which are necessary to calculate the intensity of the scattering, can be determined from Eq. (11). In this way, one may obtain the concentration autocorrelation function

$$\langle|\varepsilon(\mathbf{q})|^2\rangle=\frac{k_B T q_z^2}{D_{22}q_z^2+Kq_x^4}. \tag{21}$$

We also did numerical calculations to all the roots, and find, as we shall explain later in this paper, that the other two roots describe modes which decay too rapidly to see with our autocorrelator.

If Eq. (20) describes the only mode we can detect with our correlator, why did we see two decay times in the scattering? The reason is that when light passes through the sample at normal incidence, about 4.5% is reflected back into the sample by the second silica window, and we see scattering at both the angle θ and its complement, as illustrated in Fig. 2. The two components have the same q_x value, but the forward scattering has a much smaller q_z than does the backward scattering. Using Eq. (20), we may associate the slow and fast decays with backward- and forward-scattering geometries, respectively. The scattered intensity for this mode should be inversely proportional to the decay rate Γ, which will tend to make up for the weaker incident beam for the backward-scattered

light. However, that is not enough to explain the observed intensity ratio (the forward scattering is actually weaker). The wave vector for the backward scattering is about 85% of $2\pi/d_{eq}$, and the broadening of the Bragg peak may increase the scattering.

With the two geometries in mind, we analyzed our data using a numerical solution to Eq. (12), choosing the low-frequency mode, although when $D_{33} \geq 50D_{22}$, the numerical solution is indistinguishable from Eq. (20). We chose $K = k_c/d$, D_{22} given by Eq. (17), and $\mu = d_{eq}^2/(12\eta)$, as calculated by Brochard and de Gennes [6]. When these substitutions are made, the decay time for our concentration fluctuations depends strongly on only two parameters, k_c and d_{eq}, with a weak dependence on D_{33}. The other quantities are all known by other means. The results of fitting the forward- and backward-scattering data simultaneously, with $\eta = 0.005$ poise, are shown in Fig. 4. When d, D_{33}, and k_c were all allowed to vary we obtained $k_c = (7.0 \pm 5.0) \times 10^{-12}$ nJ or $(1.5 \pm 1) k_B T$, $d_{eq} = (170 \pm 40)$ nm, and $D_{33} = (5.6 \pm 1.4)$ Pa. The large uncertainties arise because the parameters are correlated in the fit. When we restrict d to the 180 nm obtained by Strey *et al.* [4], we find $k_c = (1.35 \pm 0.35) k_B T$ and $D_{33} = (5.3 \pm 0.8)$ Pa. It is not obvious that the expression $\mu = d_{eq}^2/(12\eta)$ should hold for crumpled bilayers; one might expect the crumpling would result in $\mu = d_{eff}^2/(12\eta)$, with $d_{eff} \leq d_{eq}$. As our data could be quantitatively represented by the simpler expression with reasonable values of the parameters, we did not introduce this extra complication.

We now come back to Eq. (20). When D_{33} is large, our fit of Eq. (20) to the data in Fig. 4 is as good as the numerical solution. It is rather insensitive to D_{33}. If we take any value of D_{33} greater than 50 Pa and allow d and k_c to vary, we obtain $d_{eq} = (210 \pm 15)$ nm and $k_c = (0.75 \pm 0.1) k_B T$ with a χ^2 only 20% larger than the best fit for all three parameters. For the parameters we found, the penetration depth $\lambda = (K/D_2)^{1/2}$ is 210 nm, and D_{22} is 0.8 Pa. Physically, for backward scattering, where q_z is large, the layer compression term dominates in the numerator of Eq. (20) and large concentration fluctuations are involved. For forward scattering, the curvature term dominates and the mode has become mostly one of layer undulation; it can still be detected in our polarization setting ($\mathbf{i} \| \mathbf{f}$) because small concentration fluctuations remain. The denominator of Eq. (20) is essentially q_z^2 multiplied by a constant in our experiment; the presence of the $\mu\eta q^4$ term makes this constant approximately 3 instead of 1, and therefore makes Γ three times smaller. This term results from the damping due to the slip flow of the water between the bilayers.

Returning to Eq. (12), we solved numerically for the other two roots; with these parameters, they had magnitudes of 10^4 sec^{-1} or greater. We also investigated the possibility that our two decay times might be the result of simply forward scattering by two different modes of Eq. (12), rather than forward and backward scattering of only the lowest frequency mode. When D_{33} is large enough and $q_x \sim q_z$, the two higher frequency modes are a pair of propagating "second sound" modes. However, for small values of D_{33}, as we apparently have here, all three roots of Eq. (12) are imaginary, and two of them are relatively low frequency. It was, in fact, possible to fit our data to forward scattering by the two lowest frequency roots of Eq. (12). The parameters we obtained this way were $d_{eq} = 200$ nm, $k_c = 0.08 k_B T$, and $D_{33} = 1.2$ Pa, which give $D_{22} = 9.5$ Pa and $\lambda = 14$ nm. These are so far from physically reasonable values that we believe our interpretation of forward and backward scattering from the low-frequency mode is the correct one.

IV. CONCLUSIONS

We have investigated the spectrum of light scattered from a homeotropically aligned highly swollen lamellar phase ($d \sim 180$ nm) in a nonionic binary system (C12E5 and water), where the Helfrich repulsion is the dominant force between bilayers to stabilize the lamellar order. At each scattering angle we observed an intensity autocorrelation function for the scattered light with two decay times. We identified these as coming from simultaneous observation of the baroclinic mode in both forward and backward scattering.

We conclude that the Brochard–de Gennes model [6] combined with Helfrich's calculation [5] of the entropic and steric interbilayer repulsion quantitatively describes dynamical behavior of the baroclinic mode of highly swollen lamellar phases of nonionic surfactants.

We found that for a highly swollen lamellar phase, it is important to consider the curvature elastic energy in calculating the dispersion relation even for the very oblique momentum transfer case. Because the interbilayer repulsion is so weak, the curvature energy leads to the interesting property that the mode relaxation speeds up as $q_\parallel$ becomes smaller. The faster forward-scattering branch in Fig. 4 is in the crossover region between the baroclinic mode for larger q_z and the decoupled undulation mode of $q_z = 0$. Finally, since the slip coefficient scales as d^2, the damping to the fluctuations of bilayers due to the water between them plays a more important role in highly swollen system.

ACKNOWLEDGMENTS

We appreciate helpful discussions with our colleague Mehran Kardar. We also appreciate Don Heiman's help in making the optical fiber connections. This research was supported by the National Science Foundation under Grant Nos. DMR-9014886 (J.D.L.) and DMR-911389 (S.S. and C.Y.Z.), and used equipment purchased in part by NSF Grant No. DMR-9022933.

TABLE I. Comparison of the notation used in this paper and by Nallet *et al.*

This paper	D_{22}	D_{23}	D_{33}	μ
Ref. [7][a]	$\bar{B}$	$c(c/\chi - C_c)$	c^2/χ	$\alpha_1/(\rho^2 c^2)$

[a]Note that c in Ref. [7] has different units from this paper.

APPENDIX

The articles by Nallet, Roux, and Prost [7] and by Lubensky, Prost, and Ramaswamy [8] give an extensive analysis of the modes of a lyotropic smectic, but use different notation. Our notation follows more closely that of the earlier article by Brochard and de Gennes [6]. In Table I we give parameters in the notation of Refs. [7] and [8] which correspond to the ones we used.

[1] D. Roux and A.-M. Bellocq, *Physics of Amphiphiles*, edited by V. Degiorgio and M. Corti (North-Holland, Amsterdam, 1985).
[2] D. Roux and C. R. Safinya, J. Phys. (Paris) **49**, 307 (1988).
[3] F. C. Larche, J. Appell, G. Porte, P. Bassereau, and J. Marignan, Phys. Rev. Lett. **56**, 1700 (1986).
[4] R. Strey, R. Schomacher, D. Roux, F. Nallet, and U. Olsson, J. Chem. Soc. Faraday Trans. II **86**, 2253 (1990).
[5] W. Helfrich, Z. Naturforsch. **33a**, 305 (1978).
[6] F. Brochard and P. G. de Gennes, Pramana, Suppl. No. **1**, 1 (1975).
[7] F. Nallet, D. Roux, and J. Prost, J. Phys. **50**, 3147 (1989).
[8] T. C. Lubensky, J. Prost, and S. Ramaswamy, J. Phys. **50**, 3147 (1989).
[9] P. C. Martin, O. Parodi, and P. S. Pershan, Phys. Rev. A **6**, 2401 (1972).
[10] J. N. Israelachvilli, *Intermolecular and Surface Forces* (Academic, New York, 1985), p. 253.